EVALUATION OF EQUIVALENT LINEARIZATION ANALYSIS METHODS FOR SEISMICALLY ISOLATED BUILDING USING LEAD-RUBBER BEARING

Nguyen Van Tu[1,*], Nguyen Xuan Dai[1], Pham Nam Phong[1]

[1]*Le Quy Don Technical University*

Abstract

The paper presents an evaluation of the linearization analysis method for isolated multi-story building structures using lead-rubber bearings (LRB) considering vertical stiffness and critical buckling load. The effective linear parameters of LRB are estimated by the single-mode spectral analysis method, calculating for a typical target spectrum by TCVN 9386:2012. A set of time history analyses is conducted on both the equivalent linear model and the bilinear model. A comparison of seismic responses between the two models is performed where the bilinear model included considering the effects of vertical stiffness and critical buckling load. The results show the conservative design in force and displacement of the isolated structure by the linearization analysis method, but non-conservative design in floor accelerations. Significantly higher displacement estimates by the linearization method may lead to over-designed bearing displacement capacity.

Keywords: *Seismic base isolation; bilinear model; equivalent linear model; isolators vertical stiffness; critical buckling load.*

1. Introduction

Seismic base isolation (SBI) is an extremely effective technique that widely used in earthquake regions to protect buildings. This technique introduces high horizontal flexibilities and an impressive damping ratio, allowing the building structure to move more independently from its foundation, minimizing the impact of earthquakes as well as the damages of the building structure [1-8].

Lead-rubber bearing (LRB) is one of the most typical SBI devices that has widely used for seismically isolated buildings. It consists of an elastomeric bearing with a central core of lead, shown in Figure 1. The LBR geometric properties include the lead diameter (d_L), bearing's total diameter (D_r), steel shim thickness (t_s), single rubber layer thickness (t_r), number of rubber layers (n_r), rubber's total thickness ($h_r = n_r.t_r$), bearing's height (rubber and steel shim) (h) and total height of the bearing included connecting plate (H). The low shear modulus of the rubber is considered the key parameter that mainly contributes to the high lateral flexibility of the bearing working in shear. The lead

* Email: nguyentu@lqdtu.edu.vn
https://doi.org/10.56651/lqdtu.jst.v3.n02.153.sce

plug, characterized by perfect plastic deformation behavior in shear, provides an excellent energy dissipation capacity. In such conditions, LRB devices provide a great equivalent damping ratio (up to 30%) and also can be easily modified by the change of the appropriate size of the lead plug [2, 9, 10].

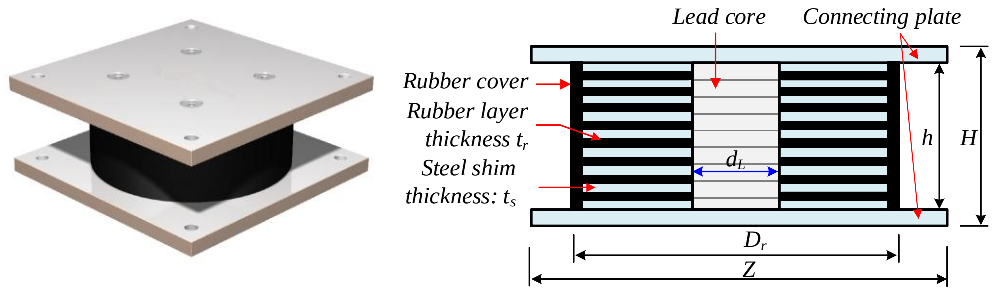

Figure 1. Lead-rubber bearing structure.

Previous researches have been conducted on the seismic response of isolated structures, based on three main analysis methods such as single-mode spectral analysis (SMSA), multi-mode spectral analysis (MMSA), and nonlinear time-history analysis (NLTHA) [2, 9, 11-14]. Among them, the NLTHA method provides the complete nonlinear response history of isolated structures, making it to be considered the most accurate method. Both the SMSA and the MMSA methods offer a more rapid alternative when the peak seismic demand in terms of displacement and force are of interest, such as for design proposes. These two methods are based on using an equivalent linear model of the isolated structures, where the effective parameters of stiffness (K_{eff}) and damping ratio (ξ_{eff}) are estimated from the expected maximum seismic displacement. Generally, the NLTHA method is required to analyze complex building structures, to validate the preliminary analyses results for the final design. The SMSA method is a static simplified procedure and particularly useful for the preliminary design and sizing of the SIS for a specific structure, which is recognized as a valid method for design in the current codes and specifications [9, 10, 13, 14]. However, the accuracy of this method is not well established. The inherent hysteresis damping of the isolators is replaced by equivalent viscous damping may lead to an erroneous estimate of the peak response and therefore need to be revisited.

On the other hand, as consequences of using SBI, the increase of structural flexibilities results in increases of lateral displacement, which occurs mostly in the bearing rather than the structural component of construction. Meanwhile, for elastomeric bearings, the effective stiffness of devices is primarily estimated from the elastic modulus of the material and its cross-sectional area. In large lateral deformations states, the seismic performance of bearings may reduce in both horizontal and vertical directions, leading to the collapse of devices with two main failure modes such as the tearing of the rubber and the buckling failure [15-17]. However, the equivalent linear model focuses on the determination of the horizontal stiffness and equivalent damping ratio without considering the horizontal-vertical coupling and buckling effects. The evaluation of the final bearing properties subjected to the combined compression and lateral deformation, therefore, is an essential part of the quantitative assessment of elastomeric bearing, especially its stability.

The effect of lateral deformation on the load-carrying capacity of isolators has been studied early and currently applied for the design of elastomeric bearing [1, 2, 16, 18]. The obtained results have shown that the increase in the axial load and the lateral displacement leads to a decrease in the critical load and the horizontal stiffness. Naeim and Kelly [2], presented the reduced area method to calculate the vertical stiffness where the reduction of the compressive cross-section during the operation of bearings was mentioned. The theory of determining the stability of LRB is based on Haringx's works to determine the stability of rubber rods [19]. Gent [20] investigated the effect of axial load on the horizontal stiffness of elastomeric bearings, predicted the critical buckling load, and verified Haringx's theory by experimental tests. It confirmed the applicability of Haringx's theory for modeling the buckling behavior of elastomeric bearing under the horizontal-vertical coupling.

In this study, the suitability of the linearization analysis method for isolated-building structures is investigated by comparisons of seismic responses between two models such as the equivalent linear model and the bilinear model. The properties of LRB are estimated by the SMSA method, where the effective parameters of isolators are preliminarily calculated based on the design spectrum of Son La, Vietnam [21], and using to select the structure of LRB. The horizontal stiffness, the vertical stiffness, and the critical buckling load are formulated and applied for the bilinear model. The design parameters are then recalculated for considered analysis cases where the vertical stiffness and critical buckling load are mentioned. A set of three earthquake records are selected and calibrated to match the target spectrum in order to perform the seismic response of isolate building by nonlinear time history analysis. Finally, a comparison of the seismic response between the two models is conducted to evaluate the accuracy of the equivalent linear analysis methods.

2. Formulations for the isolator stiffness

2.1. Horizontal stiffness

In practice, the isolation bearing is often modeled by a bilinear model with four main parameters such as the characteristic strength, Q; the post-yielding stiffness, K_2; the yield displacement, D_y; and the maximum displacement, D_{max}, as shown in Figure 2 [2].

The effective stiffness of equivalent model, K_{eff}, can be determined as follows:

$$K_{eff} = M \times \left(2\pi/T_{eff}\right)^2, \tag{1}$$

where M is the mass total of construction on the LBR (ton); T_{eff} is the effective period of the isolation system (sec).

The maximum displacement, D_{max}, can be determined from the spectral displacement given by the code as the following:

$$D_{\max} = F_{\max} / K_{eff} = MS_a\left(T_{eff}, \xi_{eff}\right) / K_{eff}, \tag{2}$$

where $S_a(T)$ is the elastic response acceleration spectrum; ξ_{eff} is the effective equivalent viscous damping ratio, expressed as a percentage.

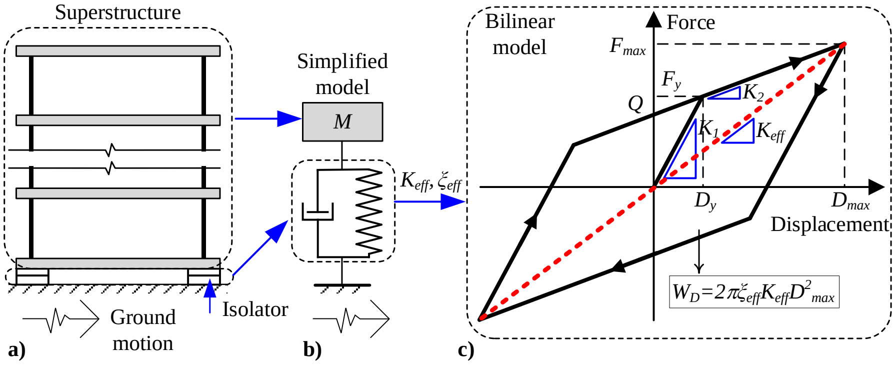

Figure 2. Simplified model of isolated building and equivalent bilinear model.

The energy dissipated per cycle (EDC) is determined by the area under hysteresis loop and considered by an equivalent linear viscoelastic system:

$$W_D = EDC = 4Q\left(D_{\max} - D_y\right) = 2\pi\xi_{eff} K_{eff} D_{\max}^2. \tag{3}$$

Therefore, the effective equivalent-damping ratio can be calculated as follows:

$$\xi_{eff} = \frac{2Q\left(D_{\max} - D_y\right)}{\pi K_{eff} D_{\max}^2}. \tag{4}$$

The initial stiffness, K_1 of equivalent model can be determined as follows:

$$K_1 = Q / D_y + K_2; K_2 = K_{eff} - Q / D_{\max}. \tag{5}$$

Because these equations are coupled with each other, it is necessary to use an iterative procedure to calculate the design parameters. Set up the calculation program SBI properties (SBIP) based on Matlab software [22].

Focusing on the application of LRB, it should be noted that the contribution of rubber components is significant to the stiffness of bearing. Meanwhile, its effects on the characteristic strength of the device (Q) (including the yield force, F_y) are relatively negligible when compared with the lead plug. Therefore, Q and F_y can be approximated only by the lead core as follows:

$$F_y = \frac{1}{\psi} f_{yL} \frac{\pi d_L^2}{4}; Q = F_y \left(1-\alpha\right), \tag{6}$$

where f_{yL} is the shear yield stress of lead, d_L is the diameter of the lead plug ($D_r/6 < d_L < D_r/3$) [11], ψ is load factor accounting for creep in lead (ψ = 1 for seismic loads), and $\alpha = K_2/K_1$ is the post-elastic ratio, taken in the range of α = [1/30÷1/15] for the lead-plug rubber bearing [2].

2.2. Vertical stiffness

In order to provide a visual physical model, the concept of the springs model is employed to investigate the mechanical properties of the elastomeric bearing subjected to the combined axial force and horizontal deformation [15, 23] that allow approximating the devices' behavior by a detailed physical model. To do so, the lateral stiffness and the vertical stiffness of the device are modeled by a horizontal spring and a rotational spring. The stiffness of springs is determined by the displacement caused by the respective load.

Accordingly, the vertical stiffness is obtained by the mechanical model using two spring elements proposed by Koh and Kelly [24] as shown in Figure 3. The vertical stiffness of the bearing is determined as:

$$K_v = K_{v0}\left(1+\frac{3A_b}{I}\times\frac{\Delta^2}{\pi^2}\right)^{-1}. \tag{7}$$

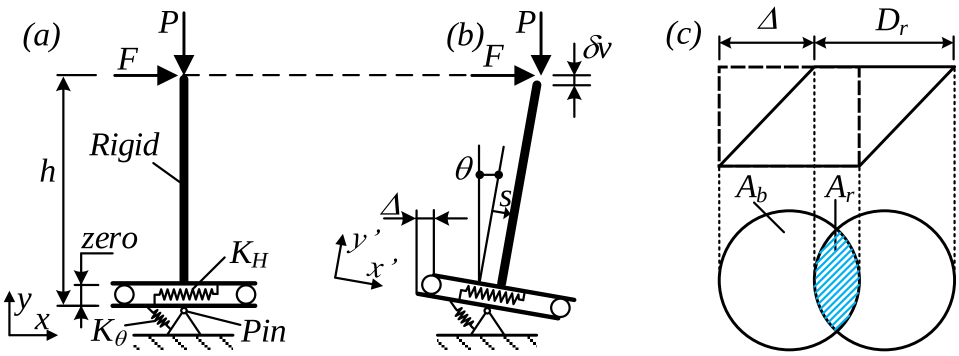

Figure 3. Two-spring model and reduction area for elastomeric bearings: (a) underformed model, (b) deformed model, and (c) notation for reduced area.

For LBR bearings as shown in Figure 1, substituting $A_b = \pi\left(D_r^2 - d_L^2\right)/4$ and $I = \pi\left(D_r^4 - d_L^4\right)/64$ into Equation (7), the vertical stiffness of LBR is determined as:

$$K_v = K_{v0} \times \left[1 + \frac{48\Delta^2}{\pi^2 \left(D_r^2 + d_L^2 \right)} \right]^{-1}, \tag{8}$$

where $K_{v0} = E_c A_b / h_r$ is the initial vertical stiffness of the bearing (without lateral displacement); A_b is the bonded rubber area; and E_c is the instantaneous compression modulus of the rubber-steel composite that is controlled by the shape factor, S, the ratios of the loaded area of rubber layer and the surrounding area on the side of a single rubber layer.

For a circular pad of diameter D_r and a single rubber layer thickness t_r:

$$E_c = 6G_r S^2; S = D_r / 4t_r. \tag{9}$$

For a square pad of side a and a single rubber layer thickness t_r:

$$E_c = 6.73G_r S^2; S = a / 4t_r. \tag{10}$$

where G_r is the shear modulus of rubber.

2.3. Buckling behaviour

The compressive cross-section of devices is considerably reduced by lateral deformation, resulting in a significant decrease in the vertical stiffness, as presented early by Buckle and Liu [25]. This concept is based on a column model with a reduced area [1, 16], as shown in Figure 3(c). Accordingly, fo the LBR subjects to a shear displacement Δ, the critical buckling load is decreased and given by the following expression:

$$P_{cr\_re} = P_{cr} \frac{A_r}{A_b} \tag{11}$$

where P_{cr_re} is the buckling load at the reduced area, P_{cr} is the buckling load at zero displacement that is determined as [24]

$$P_{cr} = \sqrt{P_E G_r A_s} \tag{12}$$

where $A_s = A_b h / h_r$; $P_E = \pi^2 E I_s / h^2$, $I_s = I \times h / h_r$; I is the moment inertia of the cross-section; E is the modulus of elasticity, $E = E_c / 3$.

For circular bearings of bounded area of diameter D_r, the reduced area A_r is calculated as:

$$A_r = \frac{D_r^2}{2} \left[\cos^{-1}\left(\frac{\Delta}{D_r} \right) - \frac{\Delta \sqrt{D_r^2 - \Delta^2}}{D_r^2} \right]. \tag{13}$$

As an observation from Equation (11), the bearing may present no capacity when the acted horizontal displacement equal to the diameter of the bearing. However, the

LBR will not lose total stability when the overlapping area is equal to zero, as observed from the experimental tests [15, 26, 27]. Therefore, an appropriate function of the reduced critical buckling load of LRB should be taken into account, as proposed formulas by Warn et al. [15]:

$$P_{crre} = \begin{cases} P_{cr}\dfrac{A_r}{A_b} & \dfrac{A_r}{A_b} \geq 0.2 \\ 0.2P_{cr} & \dfrac{A_r}{A_b} < 0.2 \end{cases} \tag{14}$$

The vertical stiffness with accounting for the reduced area is determined as follows:

$$K_v = K_{v0} \times \frac{A_r}{A_b}. \tag{15}$$

When the load carried by the LBR is comparable to the buckling load, the horizontal stiffness K_H is reduced that obtained by using the same linear analysis and is expressed as [2]:

$$K_H = \frac{G_r A_s}{h} \times \left[1 - \left(\frac{P}{P_{cr}}\right)^2\right] = K_{H0} \times \left[1 - \left(\frac{P}{P_{cr}}\right)^2\right]. \tag{16}$$

3. Numerical analysis

3.1. Description of the building structure

In this section, a set of numerical analyses for an isolated building structure is performed. A typical model 3D of a multi-story building is considered with the properties of the structure is detailed as below:

- The reinforced concrete building has 11 floors, including a basement and 10 stories. The floor height is 3.9 m for the stories and 3.6 m for the basement. The plan has three bays in the X, Y direction, as shown in Figure 4(a).

- Structural component includes: the cross-section of main beam systems is 35 cm x 75 cm (width x depth), the cross-section of sub-beam is 30 cm x 60 cm, the cross-section of foundation beam is 80 cm x100 cm. The cross-section dimensions of columns: from 1st to 4th story 100 cm x 100 cm; from 5th to 8th story 90 cm x 90 cm; from 9th to the roof 80 cm x 80 cm. The concrete wall thickness is 35 cm; and the floor thickness is 15 cm, and the basement floor is 20 cm.

- Grade of structural concrete: B35 (TCVN 5574:2018).

- Load acting: The floor loading: dead load 120 daN/m^2, live load 240 daN/m^2; the roof loading: dead load 200 daN/m^2, live load 100 daN/m^2.

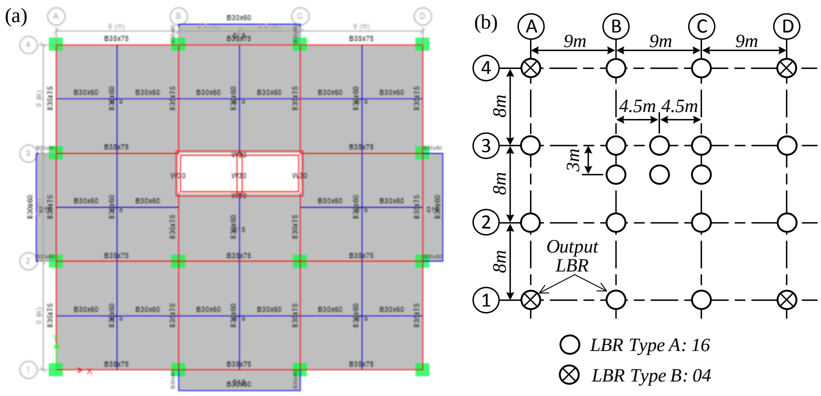

Figure 4. (a) Specific floor plan model and (b) LBR plan for design.

The designed building supports on the soil type B and located in the region of Son La, Vietnam with the design spectral acceleration according to TCVN 9386:2012, representative by a_{gR} = 0.1893 g [21]. In order to analyze nonlinear time histories isolated building, a suite of three historic ground motions is selected, shown in Table 1.

Table 1. Earthquake records selected for analyses [28].

#	Earthquake, station	Nation, date	Mw	R (km)	PGA (g)
Acc1	Chi-Chi, Taichung	Taiwan, 25-9-1999	6.3	10	0.774
Acc2	Kobe	Japan, 16-01-1995	6.9	7.1	0.509
Acc3	Northwest_China	China, 11-4-1997	6.1	27.7	0.300

Early studies have been found that no major difference in quantities of seismic response obtained from the nonlinear time history analyses using the records scaled to match the elastic design spectra and the response spectra [29-31], especially for long periods like isolated structure responses. In this study, earthquake records are scaled to match the target spectrum determined by TCVN 9386-2012 with 5% damping. There is a slight difference between the spectra of each ground motion and the target spectrum, especially for the short periods. However, the mean spectrum is found in an excellent match with the design spectra, as shown in Figure 5.

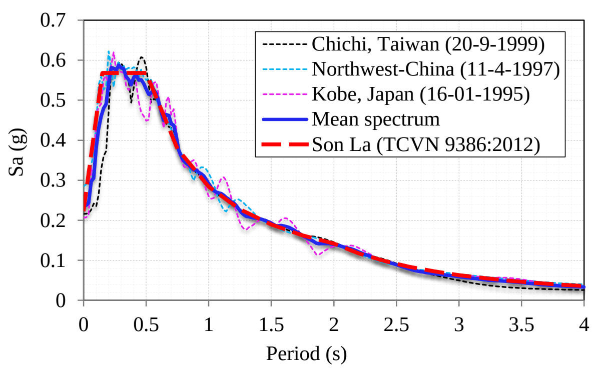

Figure 5. Ground motion time history and spectral acceleration used for study.

3.2. Design the lead rubber bearing as seismic isolation systems for building

The building is isolated by LRB systems. In the numerical model using Etabs software [32], seismic isolation systems are modeled by nonlinear link elements instead of the fixed-base constraints in the conventional structure. A total of 20 single bearing isolators (SBI) include 16 LRB devices type A and 4 LRB devices type B used for the considered building structure, shown in Figure 4(b).

With the fixed-base model, the maximum mass act on the LRB is determined such as M = 678 (ton) for one LRB type A; M = 324 (ton) for one LRB type B that use to estimate the parameters of isolators by SMSA method as shown in Figure 2. Assume that the damping ratio of isolator, ξ_{eff} = 20% (according to LRB [2]); the effective period of the fundamental mode of isolated building is assumed, T_{eff} = 2.0 s, the post-elastic ratio is α = 1/21 for analysis [2].

Based on the SBIP program, the estimated properties of two LRB types are obtained as in Table 2. Correspondingly, based on the code EN 1337-3:2005 [10] and Lead Rubber Bearings catalogue [33], selected circulars and designed parameters of each LRB type are shown in Table 3.

Table 2. Analytical properties of 2 SBI types.

SBI	M (ton)	K_{eff} (kN/mm)	K_1 (kN/mm)	K_2 (kN/mm)	Q (kN)	D_{max} (mm)	D_y (mm)
Type A	678	6.69	76.90	4.52	193	89.25	2.67
Type B	324	3.20	36.77	2.16	92	89.25	2.67

Table 3. Selected sizes for 2 SBI types.

SBI	D_r (mm)	d_L (mm)	h_r (mm)	h (mm)	H (mm)
Type A	750	250	75	95	189
Type B	500	165	50	66	160

The material parameters of rubber and lead are taken as G_r = 0.9 MPa and f_{yL} = 9 MPa. Based on the dimensions for the two types of LRB in Table 3, the parameters for devices, representative by the link elements in Etabs software, are recalculated for both analysis cases. The obtained results are represented in Table 4.

Table 4. Design parameters of SBI parameters of the element.

LBR	K_{eff} (kN/mm)	C_{eff} (kNs/mm)	D_y (mm)	F_y (kN)	D_{max} (mm)	F_{max} (kN)	K_v (kN/mm)	C_v (kNs/mm)
Case 1: Equivalent linear model								
Type A	7.880	0.985	-	-	-	-	∞	∞
Type B	5.180	0.532	-	-	-	-	∞	∞
Case 2: Nonlinear (Bilinear) model								
Type A	-	-	6.11	499	150	1160	3712	5.35
Type B	-	-	4.07	213	100	508	2475	2.91

4.3. Results and discussions

The hysteresis responses of isolators are illustrated in Figure 6 for two typical isolators type A and type B, corresponding to axis 1-A and 1-B, respectively. Practically, the drift of building structures occurs mainly at the isolators' level, corresponding to the fundamental modal of vibration. Therefore, isolators produce the same horizontal displacement that is equal to the lateral displacement at the base of the building, as shown in Figure 6. In such contexts, the seismic response of the isolator at axis 1-A (type A) is selected as a typical location to investigate the research goals in the next sections.

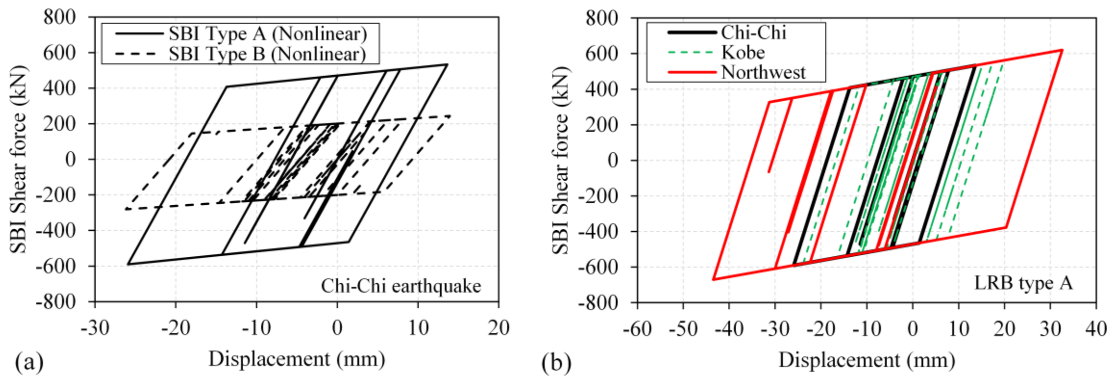

Figure 6. Hysteresis responses of isolators,
(a) Chi-Chi earthquake scaled record, (b) three considered ground motions.

Figure 7 shows the comparison of the force-displacement relationship of isolators type A between the equivalent linear model and the bilinear model. As observations from the figure, the maximum values of force and displacement calculated by the linear equivalent model is considerably higher than the bilinear model, suggesting the conservative design of isolated building structures when using the linearization analysis method. That is more detailed in time history responses of the shear force and the lateral displacement, shown in Figure 8(a) and 8(b), respectively.

These obtained results deem to be a consequence of the SBI calculation by the equivalent linear model. While the earthquake, by the ground motion acceleration, impacts the building mass that producing the lateral inertial force nearly constant, which is proportional to the acceleration and mass. The equivalent linear model provides K_{eff} large than K_2 (post-elastic state), but much lower than K_1 (initial elastic state) of isolators. Therefore, the obtained displacement by the equivalent linear model is much larger than the bilinear model, especially in the context that the post-elastic deformation ratio of isolators [(D_{max}- D_y) / D_y] is not too large.

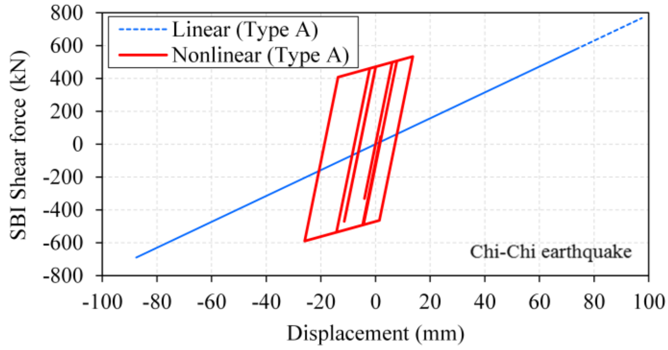

Figure 7. Comparison of force-displacement relationship between equivalent linear model and bilinear model.

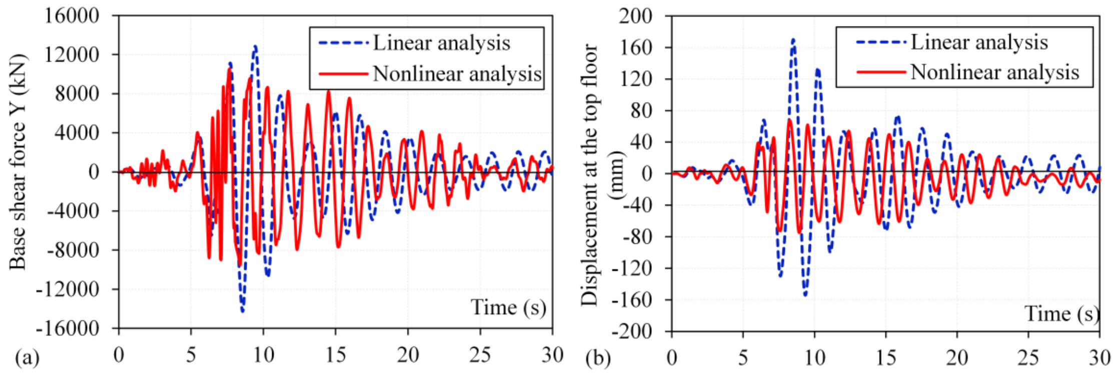

Figure 8. Time history responses of base shear forces (a) and lateral displacements at top story (b) Son La, Vietnam earthquake with Chi-Chi scaled record.

Figure 9 and 10 show the comparisons of peak responses in the displacement, the base shear force, and the top floor acceleration. The results indicate that the predictions of the displacement and the shear force by the equivalent linear model are significantly higher than the nonlinear model, allowing a guarantee of conservative designs for structural components. However, the too much higher estimates of displacement by the equivalent linear model, especially at the base of the building structure, may lead to over-designed displacement capacity of bearings that strongly influence the sizing of devices as well as the economical design. The underestimates of the top floor acceleration by the equivalent linear model is due to the linearization method lead to much higher of K_{eff} of the equivalent linear model than the post-elastic stiffness of LRB in the plastic regime. As shown in Table 5, the difference of predictions in base displacement and floor accelerations between the equivalent linear model and bilinear model is up to more than 65%, suggesting a considerable inaccuracy may occur in the application of the linearization approach.

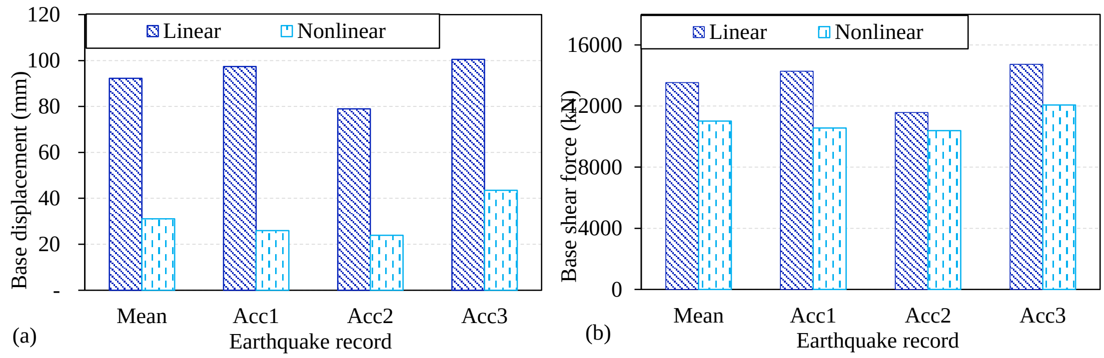

Figure 9. Comparison of peak responses in base displacement and base shear forces.

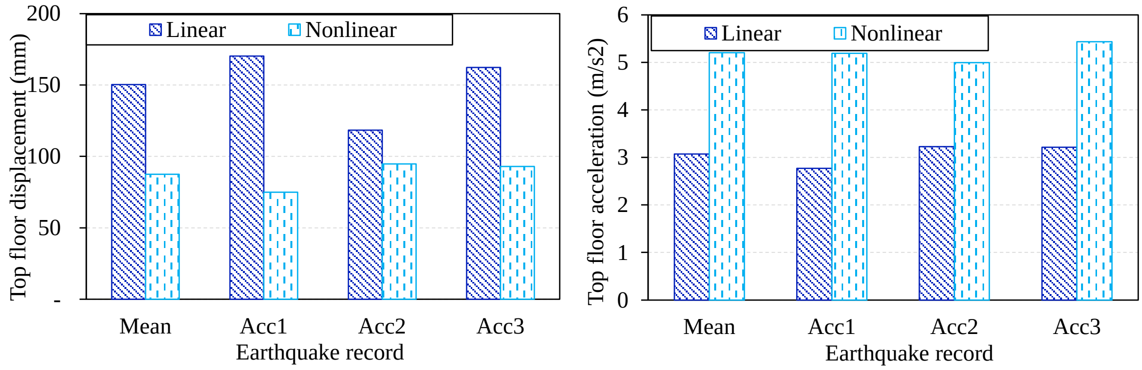

Figure 10. Comparison of peak responses in top floor displacement and acceleration.

Table 5. Comparisons of mean seismic responses between cases analyzed.

Mean seismic response	Case 1 (1)	Case 2 (2)	Compare ((1)-(2)) / (1)| (%)
Base displacement (mm)	92.29	31.09	66.31
Base shear force (kN)	13533	11011	18.63
Top floor displacement (mm)	150.28	87.54	41.75
Top floor acceleration (m/s^2)	3.07	5.21	-69.52

5. Conclusions

In this paper, a numerical study of the seismically isolated building structure is presented through time history analyses via two models such as equivalent linear and bilinear. The equivalent linear model properties of bearings are estimated by the single modal spectral analysis method, where the horizontal stiffness and the equivalent-damping ratio are mentioned. The nonlinear model properties of bearings include the bilinear hysteresis for horizontal behavior, the vertical stiffness, and the effects of the critical buckling load. The results show that the predictions seismic responses of building structures by equivalent linear model present overestimates in shear forces and displacements, but underestimates of floor accelerations. This difference suggests a considerable effect of vertical stiffness and critical buckling load as well as the replacement of the bilinear behavior of SBI by the equivalent linear model on the seismic responses of isolated structures. Furthermore, significant differences in the predictions of base displacements and floor accelerations require some cautions in applying the equivalent linear models for SBI.

References

1. Kelly J M (1993). *Earthquake-Resistant Design with Rubber,* Springer-Verlag.
2. Naeim F and Kelly J M (1999). *Design of Seismic Isolated Structures: From Theory to Practice,* John Wiley & Sons, Inc.
3. Sahu G and Sahu P (2019). *Comparative Analysis of Effects of Base Isolator & Fluid Viscous Damper on Response of a RCC Structure*, 94-101.
4. Chopra A K (2017) *Dynamics of structures. Theory and applications to earthquake engineering,* Prentice Hall.
5. Warn G P and Ryan K L (2012). A review of seismic isolation for buildings: Historical development and research needs. *Buildings, 2*, 300-25.
6. Makris N (2019). Seismic isolation: Early history. *Earthquake Engineering & Structural Dynamics, 48*, 269-3.
7. Nath S, Debnath N and Choudhury S (2018). Methods for Improving the Seismic Performance of Structures - A Review. *IOP Conference Series: Materials Science and Engineering, 377.*
8. Shevale S S, Kadam S S, Pise C P, Pawar Y P, Deshmukh C M and Mohite D D (2016). Seismic behaviour of multi-storied building by using tuned mass damper and base isolation: A Review. *Journal of Engineering Research and Application, 6*, 1-6.
9. AASHTO (2014). *Guide Specifications for Seismic Isolation Design*, Washington, DC.
10. EN 1337-3:2005. *Structural Bearings - Part 3: Elastomeric bearings,* CEN.
11. Buckle I G, Constantinou M C, Dicleli M and Ghasemi H (2006). *Seismic Isolation of Highway Bridges,* MCEER, University at Buffalo, the State University of New York.
12. Kazeminezhad E, Taghi M and Mirhosseini S M (2020). Modified procedure of lead rubber isolator design used in the reinforced concrete building. *Structures, 27*, 2245-73.
13. EN 1998-1 Eurocode 8 (2005). *Design of structures for earthquake resistance. Part 1: General rules, seismic actions and rules for buildings*. CEN.
14. ASCE/SEI 7-10 2010. *Minimum Design Loads for Buildings and Other Structures,* Reston, VA.
15. Warn G P, Whittaker A S and Constantinou M C (2007). Vertical Stiffness of Elastomeric and Lead - Rubber Seismic Isolation Bearings. *Journal of Structural Engineering, 133*, 1227-36.

16. Buckle I G, Itani A and Monzon E (2017). Stability of elastomeric isolation systems. *NZSEE Conference,* pp. 0-7.
17. Yang T Y and Zhang H (2019). Seismic Safety Assessment of Base-Isolated Buildings Using Lead-Rubber Bearings. *Earthquake Spectra, 35*, 1087-108.
18. Nagarajaiah S and Ferrell K (1999). Stability of elastomeric seismic isolation bearings. *Journal of Structural Engineering, 125*, 946-54.
19. Haringx J A (1948). On highly compressible helical springs and rubber rods, and their application for vibration-free mountings. *Philips Research Reports.*
20. Gent B A N (1964). Elastic stability of rubber compression springs. *Journal Mechanical Engineering Science, 6,* 318-26.
21. TCVN 9386 2012. *Thiết kế công trình chịu động đất, Phần 1.*
22. The MathWorks Inc. 2017, *Matlab*.
23. Koh C G and Kelly J M (1987). *Effects of Axial Load on Elastomeric Isolation Bearings,* University of California, Berkeley, CA: Earthquake Engineering Research Center.
24. Koh C G and Kelly J M (1988). A simple mechanical model for elastomeric bearings used in base isolation. *International Journal Mechnical Science, 30*, 933-43.
25. Buckle I G and Liu H (1993). Stability of elastomeric seismic isolation systems. *Proceedings of the Seminar on Seismic Isolation, Passive Energy Dissipation, and Control,* Redwood City, California, pp. 293-305.
26. Sanchez J, Masroor A, Mosqueda G and Ryan K (2013). Static and Dynamic Stability of Elastomeric Bearings for Seismic Protection of Structures. *Journal of Structural Engineering, 139*, 1149-59.
27. Weisman J and Warn G P (2012). Stability of Elastomeric and Lead-Rubber Seismic Isolation Bearings. *Journal of Structural Engineering (United States), 138,* 215-23.
28. CESMD 2020 The Center for Engineering Strong-Motion Data.
29. Ucar T and Merter O (2019). Effect of design spectral shape on inelastic response of RC frames subjected to spectrum matched ground motions. *Structural Engineering and Mechanics, 69*, 293-306.
30. Samanta A and Pandey P (2018). Effects of ground motion modification methods and ground motion duration on seismic performance of a 15-storied building. *Journal of Building Engineering, 15*, 14-25.
31. Pant D R and Maharjan M (2016). On selection and scaling of ground motions for analysis of seismically isolated structures. *Earthquake Engineering and Engineering Vibration, 15,* 633-48.
32. *CSI 2018 Etabs Version 17.0.1*
33. Alga Spa (2008). *High damping rubber bearings and Lead Rubber Bearings Catalogue*.

ĐÁNH GIÁ PHƯƠNG PHÁP PHÂN TÍCH TUYẾN TÍNH TƯƠNG ĐƯƠNG TRONG TÍNH TOÁN CÔNG TRÌNH CÁCH LY ĐỊA CHẤN BẰNG GỐI CAO SU LÕI CHÌ

Tóm tắt: *Bài báo trình bày nội dung đánh giá về phương pháp phân tích tuyến tính đơn giản đối với các kết cấu nhà nhiều tầng cách chấn đáy bằng gối cao su lõi chì (LRB) có kể đến độ cứng dọc trục và lực dọc tới hạn của thiết bị. Các tham số tuyến tính tương đương của LRB được ước tính bằng phương pháp phân tích tuyến tính đơn giản với phổ mục tiêu điển hình theo TCVN 9386:2012. Các phân tích theo lịch sử thời gian được thực hiện trên cả mô hình tuyến tính tương đương và mô hình song tuyến. Nội dung so sánh các phản ứng động đất giữa hai mô hình được phân tích, trong đó mô hình song tuyến tính có kể đến các ảnh hưởng của độ cứng dọc trục và lực dọc tới hạn của thiết bị. Kết quả cho thấy, theo phương pháp phân tích tuyến tính tương đương, kết cấu cách chấn đảm bảo an toàn về lực và chuyển vị, nhưng thiếu an toàn đối với gia tốc tại các mức sàn. Các ước tính chuyển vị cao hơn đáng kể theo phương pháp tuyến tính tương đương có thể dẫn đến việc thiết kế dư khả năng chuyển vị của gối cách chấn.*

Từ khóa: Cách ly địa chấn đáy; mô hình song tuyến tính; mô hình tuyến tính tương đương; độ cứng dọc trục; lực dọc tới hạn.

Received: 16/10/2020; *Revised:* 26/11/2020; *Accepted for publication:* 23/12/2020

❑